



## TWELVE-DAY MEDIUM PUMPING INTO TUBULAR CELL-LADEN SCAFFOLD USING A LAB-MADE PDMS CONNECTOR

V-T. Duong<sup>1</sup>, T-T. Dang<sup>2</sup>, J.P. Kim<sup>3</sup>, K. Kim<sup>4</sup>, H. Ko<sup>5</sup>, C.H. Hwang<sup>6</sup>, K-i. Koo<sup>1,\*</sup>

<sup>1</sup> Department of Biomedical Engineering, University of Ulsan, Ulsan, Republic of Korea

<sup>2</sup> Department of Biological Science, University of Ulsan, Ulsan, Republic of Korea

<sup>3</sup> Mobile Healthcare Laboratory, Samsung Advanced Institute Technology, Suwon, Republic of Korea

<sup>4</sup> Department of Electronics and Control Engineering, Hanbat National University, Daejeon, Republic of Korea

<sup>5</sup> Department of Electronics, Chungnam National University, Daejeon, Republic of Korea

<sup>6</sup> Department of Physical Medicine and Rehabilitation, Ulsan University Hospital, University of Ulsan College of Medicine, Ulsan, Republic of Korea

### Abstract

In the current study, a method is proposed to supply culture medium into a two-layered cell-laden tubular scaffold in order to enhance cell proliferation, confluence, and viability. The two-layered cell-laden tubular scaffold was made of calcium-alginate mixed with fibroblast cells (NIH/3T3) using a lab-made double-coaxial laminar-flow generator. Afterwards, the tubular scaffold was connected to a syringe pump system using a polydimethylsiloxane (PDMS) micro-connector for long-term cell culture. Three medium pumping conditions were applied and compared: a heart-beat-mimicking pumping (20  $\mu$ L/s, 1 s period, and 50 % pulse width), a continuous pumping (20  $\mu$ L/s) and a non-pumping. Non-leaky connections between the tubular scaffolds and the micro-connector outlet were sustained for  $13.5 \pm 0.83$  d in heartbeat-mimicking pumping and  $11.8 \pm 0.33$  d in continuous pumping condition, due to the elasticity of the tubular scaffolds. Importantly, the two pumping conditions resulted in more cell proliferation, confluence, and viability than the non-pumping condition. Furthermore, analysis of newly-produced type-I collagen matrix indicated that the cells under the two pumping conditions formed a tissue-like structure. The proposed technique could further be applied to vascular co-culturing for vascular engineered tissue.

**Keywords:** Two-layered cell-laden, calcium-alginate, double-coaxial generator, fibroblast, long-term culturing, media pumping.

**\*Address for correspondence:** Kyo-in Koo, Department of Biomedical Engineering, University of Ulsan, Ulsan, Republic of Korea. room 409, building 18, University of Ulsan, 93 Daehak-ro, Nam-gu, Ulsan (44610), Republic of Korea.

Telephone number: +82-52-259-1408 Fax number: +82-52-259-1360 Email: kikoo@ulsan.ac.kr

**Copyright policy:** This article is distributed in accordance with Creative Commons Attribution Licence (<http://creativecommons.org/licenses/by-sa/4.0/>).

### Introduction

One of the ultimate goals of tissue engineering is to replace incurable tissue by engineered biological material, so-called artificial tissue. Various technologies have been introduced, ranging from cell aggregation techniques to three-dimensional (3D) bio-printing (Landers *et al.*, 2002; Vacanti and Langer, 1999).

Despite the potential of these technologies, several challenges still remain to produce thick and complex tissues. One of them is the difficulty in supplying oxygen and nutrients (Vacanti and Langer, 1999). Because of diffusion limitation,

such tissues over a few hundred  $\mu$ m thick do not easily survive and proliferate (Folkman, 1995). Constructing an appropriate vascular structure to supply nutrient and oxygenated medium through the embedded vascular structure is critical to maintaining viable thick tissue. In the early days, some approaches where engineered tissue with a vascular structure was implanted immediately following assembly led to incorporation without any further process (White *et al.*, 2014). Nowadays, most strategies include an *in vitro* culturing step to differentiate the mass of cells into functional tissue for rapid *in vivo* integration after the implantation (Miller

*et al.*, 2012). Therefore, supplying the suitable medium *in vitro* is as essential as constructing the vascular structure.

Some groups have reported the presence of perfusable micro-channels and networks inside microfluidic chips (Kim *et al.*, 2013; Kim *et al.*, 2016a; Kim *et al.*, 2016b; Nguyen *et al.*, 2013; Yeon *et al.*, 2012). Angiogenic sprouting was reconstructed inside a microfluidic chip to form vascular networks. Unfortunately, such artificial networks are impossible to harvest from the microfluidic chips for implantation (Srigunapalan *et al.*, 2011).

Jeong *et al.* (2004) introduced a microfluidic spinning method. This technique inspired others to develop a chip-free tubular cell-laden scaffold (Duong *et al.*, 2018; Jung *et al.*, 2014; Oh *et al.*, 2015; Onoe *et al.*, 2013). The generated scaffold works as a cradle for the embedded cells. With time, building material, usually hydrogel, gradually degrades and the embedded cells proliferate. The proliferated cells secrete extra-cellular matrix (ECM) material to replace the degraded scaffold material and adhere tightly to it (Onoe *et al.*, 2013). By this procedure, the composed cell-laden scaffold becomes a functionalised tissue.

A practical medium-supplying system requires a simple installation as well as a long-term secure connection. Several methods have been proposed: a simple immersion in culture medium (Duong *et al.*, 2018; Oh *et al.*, 2015; Onoe *et al.*, 2013), supplying a chamber for the mm-diameter tubular scaffold (Lee *et al.*, 2014), plasma-treating and anchoring the chip (Mori *et al.*, 2017), and 3D hydrogel printing of a microchannel network inside the connecting chamber (Zhang and Larsen, 2017). Using only natural diffusion during immersion could result in non-uniform cell differentiation and proliferation through the 150 µm thick wall. Both the flow chamber and the plasma-treated anchoring chip were complicated to fabricate and could not infuse into microscopic channels so that the inner diameters of their channels were over 700 µm and 500 µm, respectively.

In this study, cell medium was supplied into a microscopic tubular cell-laden scaffold for around 12 d, using three different pumping conditions, through a polydimethylsiloxane (PDMS) micro-connector. The PDMS micro-connector consisted of one outlet for the scaffold and one inlet for a syringe pump. Negative pressure by the inlet-connected syringe pump sucked the scaffold into the outlet. The elasticity of the thus attached calcium alginate scaffold maintained a secure connection for 11–14 d. The syringe pump supplied cell medium into a centre channel of the tubular scaffold through the PDMS micro-connector.

To minimise the effect of medium diffusion from outside of the tubular scaffolds, a two-

layered tubular scaffold was made using a double-coaxial laminar flow generator. The inner layer embedding the centre channel contained NIH/3T3 cells. On the other hand, the outer layer had no cells. The hydrogel-only outer layer hindered the medium in the outer layer from diffusing into the cells of the inner layer. Due to this diffusion-barrier layer, the cells embedded in the inner layer could only be supplied through the central hollow channel of the scaffold. Three pumping conditions (heartbeat-mimicking pumping, continuous pumping, and non-pumping) were configured and the results compared. After 20 d of culturing, the scaffolds produced under these three pumping conditions were analysed and compared for cell viability, cell proliferation, cell-cell contacts, as well as secretion of ECM material.

## Materials and Methods

### PDMS double-coaxial laminar flow generator

In order to investigate the role of a channel to supply cell medium to cells in a scaffold, it was necessary to decrease the effect of all other medium diffusion paths except for that channel. Even though hydrogel material is usually porous to small molecules and is water-permeable, if sufficiently thick it is expected to minimise cell medium diffusion from the outside to the cells (Hannoun and Stephanopoulos, 1986). A double-coaxial laminar flow generator was fabricated with a hydrogel-only outer layer and a cell-and-hydrogel inner layer embedding the medium-supply channel, as shown in Fig. 1a-f. The generator consisted of three glass inlets (Internal diameter (ID) 580 µm, G100-3, Warner Instruments LLC, U.S.A.) and one outlet (ID 1160 µm, G200-6, Warner Instruments LLC, U.S.A.). Cross-linking material was injected through the first inlet which became the central channel. The mixture of hydrogel material and cells was infused through the second inlet as an inner layer. Hydrogel-only material wrapped the inner layer through the third inlet as an outer-barrier layer. All of these glass capillaries were assembled in two cuboid-shaped PDMS blocks which were fixed on a microscope glass slide (26 × 76 × 1 mm, 1000412, Marienfeld, Germany) (Fig. 1a-b). The three inlets were treated under the heat-drawing process with a PC-10 puller (NARISHIGE Group, U.S.A.) to be automatically pulled to reach an inner diameter of about 200 µm with a tapering shape, prior to assembling on the PDMS block (Fig. 1c). Fig. 1d shows the outlet of the generator. The two PDMS blocks were fabricated by coagulating the silicone elastomer mixture (Dow Corning Corporation, Midland, U.S.A.) onto a partially-pulled glass capillary. After the heat-gelation process, the partially-

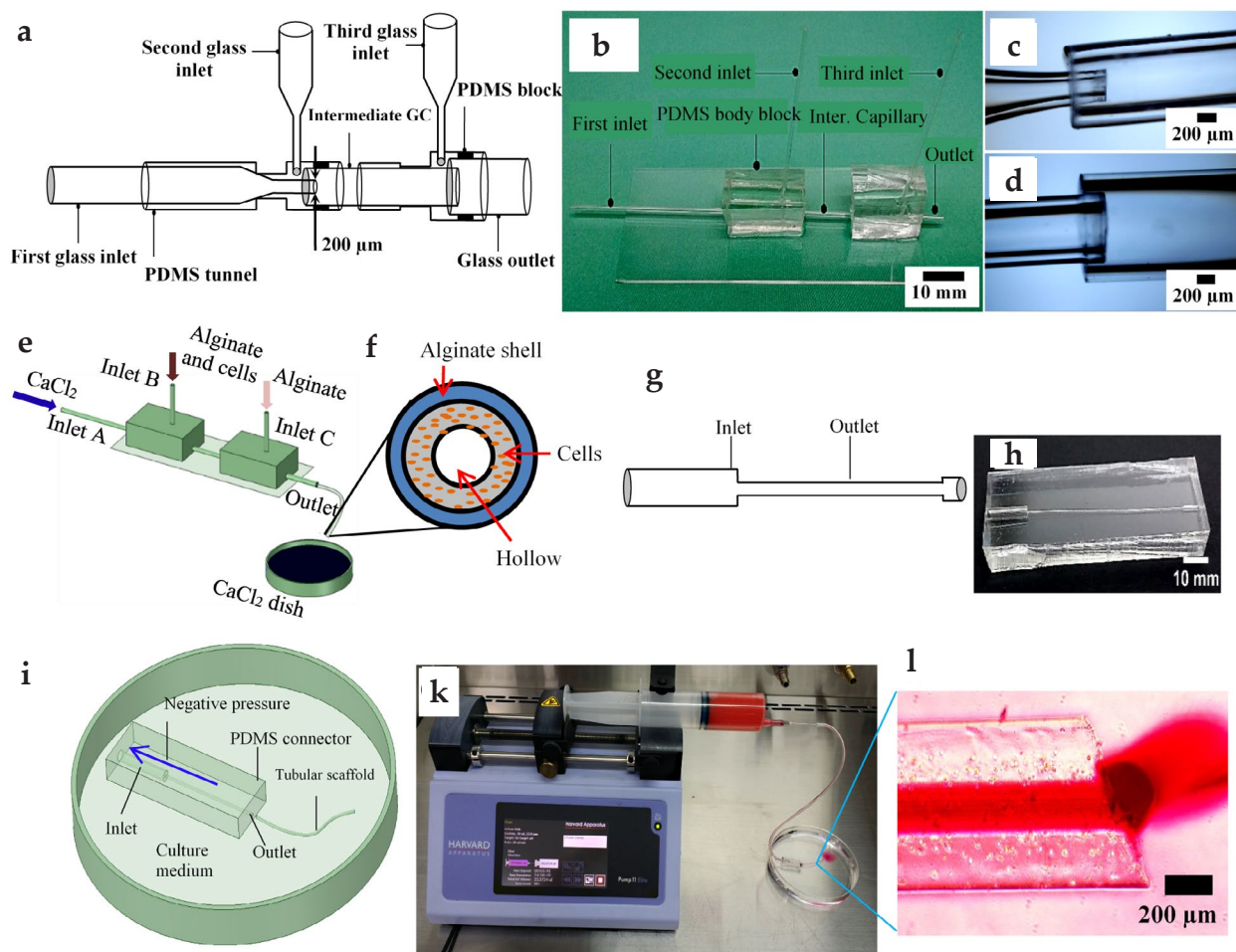


**Fig. 1. The device fabrication and experimental configuration.** (a) Illustration of the double-coaxial laminar flow microfluidic generator. The generator consists of three inlets, one intermediate glass capillary, and one outlet. (b) The fabricated generator. The inlets, intermediate glass capillary, and outlet are assembled using 2 PDMS block and fixed onto a microscope glass. (c-d) The microscopic observation of the intersectional points between the inlets and the intermediate glass capillary as well as between the intermediate glass capillary and the outlet. (e) The concept of scaffold forming. The NIH/3T3 calcium-alginate 2-layered hydrogel scaffold was continuously generated in a PDMS double-coaxial laminar flow generator before completing the outside gelation in a  $\text{CaCl}_2$  dish. (f) The scaffold's structure consists of one outside calcium-alginate layer, and one inside NIH/3T3 calcium-alginate layer. The hollow was formed by crosslinking activity at the intersectional point between inlet A and inlet B in the generator. (g) The schematic of the PDMS connector. (h) The fabricated PDMS connector. (i) The conceptual schematic of inserting the scaffold into the outlet of the PDMS connector. (j) The food dye leakage test for the syringe pump, PDMS connector and tubular scaffold. (l) The outflowing of food dye through the end of the connected tubular scaffold.

pulled glass capillaries were replaced by the inlet glass capillaries, the intermediate glass capillary, and the outlet capillary, respectively, for secure connections. The fabricated generator was sterilised at 121 °C for 15 min.

### Cell culture

Fibroblast cells (NIH/3T3, CRL-1658, cryopreserved) were purchased from a commercial source (ATCC, U.S.A). The cell vial was thawed and incubated at 37 °C in a cell incubator containing 5 %  $\text{CO}_2$ . During expansion, NIH/3T3 cells were supplied with full cell-culture media (90 % DMEM + 10 % FBS + 1 % penicillin/streptomycin). The cells were passaged before reaching 80 % confluence using 0.05 % trypsin/

EDTA solution. The cells within passage 10 ~ 17 were used in experiments.

### Two-layered tubular scaffold formation

The two-layered tubular scaffold was produced using the fabricated double-coaxial laminar flow generator (Fig. 1e-f). Sterilised 200 mM calcium chloride dihydrate ( $\text{CaCl}_2$ ) solution (223506, Sigma-Aldrich, U.S.A.) was injected into the inlet A with 120  $\mu\text{L}/\text{min}$  of flow rate for the central hollow channel. A mixture of sterilised 1.5 wt% sodium alginate solution (W201502, Sigma-Aldrich, U.S.A.) and NIH/3T3 (ATCC, U.S.A.) cells were pumped into the inlet B with a 250  $\mu\text{L}/\text{min}$  of flow rate for the cell-laden inner layer. Cell density in the sodium alginate mixture

was adjusted to about  $0.8 \times 10^6$  cells/mL. Due to chemical crosslinking between sodium alginate and  $\text{CaCl}_2$  at the intersectional point of these two inlets, a hollow was formed inside the inner layer. The ID of the central channel ranged from 160  $\mu\text{m}$  to 230  $\mu\text{m}$ , depending on the flow rate of the  $\text{CaCl}_2$  and the mixture solution. Sterilised 0.5 wt% sodium alginate solution was infused into the inlet C with a 300  $\mu\text{L}/\text{min}$  of flow rate for the hydrogel outer layer only. The double-coaxial laminar material arrived through the outlet and was maintained at a 200 mM  $\text{CaCl}_2$  in a Petri dish for 2-5 min to complete gelation process.

### PDMS connector

In order to make a secure connection between a macro medium pump and a microtubular scaffold, a connector utilising elasticity of the connecting components was designed (Fig. 1g). The connector consisted of one inlet for the connection to a syringe pump (11 Elite C300918, Harvard Apparatus, U.S.A.) and one outlet for the scaffold mounting. The diameter of the inlet and the outlet was designed to be smaller than those of the connecting components (a plastic tube and the tubular scaffold). In case of the outlet, its length was more than one hundred times its diameter for the enduring connection. The connector was fabricated from PDMS using a 550  $\mu\text{m}$  outer diameter needle (24G, KOVAX-NEEDLE, Korea Vaccine, Korea) as a mould (Fig. 1h). For the outlet formation, the PDMS solution mixture was poured on the needle mould. After curing at 60 °C for 4 h, the needle mould was removed. The fabricated connector was also autoclaved before use.

A 640  $\mu\text{m}$ -inner-diameter plastic tube (Tygon E-Lab extension tubing, Harvard Apparatus, U.S.A.), which was connected to a syringe pump, was inserted into the inlet of the PDMS connector. Due to the negative pressure from the connected syringe, the PDMS connector sucked a 70 mm-long scaffold into the outlet (Fig. 1i). Usually, the tubular scaffold was sucked up to a position about 30 mm from the outlet point. Fig. 1k,l show that food dye supplied from the syringe pump flowed out through the end of the connected tubular scaffold.

### Medium pumping configuration

According to the previous reports (Riva *et al.*, 1985; Tao *et al.*, 2009; Wang *et al.*, 2007), blood flow velocity in human blood vessels in the diameter range 100-1000  $\mu\text{m}$  is about 15-50  $\mu\text{L}/\text{min}$ . To mimic the *in vivo* environment (blood flow velocity and heart beating), culture medium was pumped at a flow rate of 20  $\mu\text{L}/\text{min}$ , for a period of 1 s and 50 % pulse width. In order to compare the effect of the heart beating and the medium pumping on time elapsed before loosening and cell proliferation, a continuous pumping condition (20  $\mu\text{L}/\text{min}$  flow rate) and

a non-pumping condition were employed as well. Under the non-pumping condition, the cell scaffolds were simply soaked in culture medium without any connection. All the scaffolds of the three conditions were incubated at 37 °C and 5 %  $\text{CO}_2$ . The medium in the scaffold and the pump was exchanged for fresh medium every 24 h.

### Cell staining

The alginate cell scaffolds were stained in 1 × phosphate buffered saline (PBS) (D8662-500ML, Sigma-Aldrich, U.S.A.) solution containing 0.2 % ethidium homodimer (1 : 2 mM) in dimethyl sulphoxide (DMSO)/ $\text{H}_2\text{O}$  1 : 4 (v/v); 0.05 % calcein-acetoxyethyl (calcein-AM) 4 mM in anhydrous DMSO (LIVE/DEAD Viability/Cytotoxicity Kit for mammalian cells, Molecular Probes, U.S.A. or fluorescein, Novartis, Switzerland). The nuclei of cells were stained using 4',6-diamidino-2-phenylindole (DAPI, NucBlue® Live ReadyProbes™ Reagent, Thermo Fisher Scientific, U.S.A.) for 30 min using an incubating condition of 37 °C and 5 %  $\text{CO}_2$ .

### Immunocytochemistry for cadherin

A tubular cell scaffold was immersed in a 0.5 % native-collagen dish and incubated at 37 °C for 15 min for gelation. This process prevented the scaffold from breaking down due to liquid flow during the exchange of solutions needed for immunocytochemistry procedures. All the reactions with the cell scaffold were conducted by diffusion through the collagen barrier. After the gelation of the collagen layer, the cell scaffold was fixed for 1 h with 4 % paraformaldehyde (P6148 Sigma-Aldrich, U.S.A.) in 1 × PBS at room temperature (RT), then permeabilised with 0.5 % Triton™-X100 (X100 Sigma-Aldrich, U.S.A.) in 1 × PBS for 5 min at RT and blocked with 5 % skim milk (70166 Sigma-Aldrich, U.S.A.) in 1 × PBS containing 0.2 % Tween 20 (P1379 Sigma-Aldrich, U.S.A.) for 1 h at 37 °C. The cell scaffold was then treated, at 4 °C overnight, with mouse anti-pan cadherin antibody (CH-19) (1 : 100, ab6528, Abcam, U.K.), followed by a 1 h incubation in Alexa Fluor 594™-conjugated goat anti-mouse IgG secondary antibody (Invitrogen, U.S.A.) and DAPI (1  $\mu\text{g}/\text{mL}$ , D1396, Invitrogen, U.S.A.) for nucleus staining.

### Immunocytochemistry for newly-produced type I collagen

The cell scaffold was fixed for 30 min with 4 % paraformaldehyde in 1 × PBS at RT, then permeabilised with 0.2 % Triton-X100 in 1 × PBS for 5 min at RT and blocked with 5 % skim milk in 1 × PBS for 30 min at 37 °C. The cell scaffold was then reacted with rabbit anti-mouse type I collagen antibody (1 : 200, ab21286, Abcam, U.K.) at 4 °C overnight, followed by a 1 h incubation with Alexa Fluor 594-conjugated goat anti-rabbit

IgG secondary antibody (Invitrogen, U.S.A.), and DAPI for nucleus staining.

### Microscopic imaging and analysing

The cell-stained scaffolds were observed under the IX53 inverted fluorescent microscope (Olympus, Japan) and the images were captured using the CellSens software (Olympus, Japan). For three-dimensional imaging, the FLUOVIEW FV1200 laser scanning confocal microscope (Olympus, Japan) was utilised. The live/dead cell images, the cell-cell contacts images, and the newly-produced type-I collagen matrix images of the cell scaffolds were analysed using the ImageJ 1.51h software (National Institutes of Health, U.S.A.).

### Quantification methods

Cell viability was determined using a ratio calculation between mean grey value (gv) of 2 colour channels (green for live cells and red for dead cells) on a black background. The grey values were obtained from  $10 \times$  confocal images, which were split into 2 separate colour channels using ImageJ 1.51h. Calculation was carried out according to the following equation:

$$\text{Cell viability} = \frac{100 \times \text{green gv}}{\text{green gv} + \text{red gv}}$$

The three-dimensional contour of individual cell groups was recognised among the green-stained 3D confocal images using the 3D Object Counter v2.0 tool of the ImageJ 1.51h. The volume of every contoured cell group was also calculated using the same tool. One NIH/3T3 cell was assumed to have an  $8,000 \mu\text{m}^3$  volume ( $20 \times 20 \times 20 \mu\text{m}$ ). The number of cells in every contoured cell group was estimated based on this assumption.

### Statistical analysis

Results are presented as mean  $\pm$  standard deviation. Statistical significance was calculated using two-tailed student's *t*-test in Microsoft Excel of Microsoft Office 365 ProPlus, where \**p* < 0.05; \*\**p* < 0.01; \*\*\**p* < 0.001. Six samples from 2 experiments were statistically analysed for the cell grouping comparison. Eight samples from 3 experiments were analysed for the cell viability comparison.

## Results

### Construction of the vascular structure with a diffusion restricting barrier

The two-layered cell-laden tubular scaffold was produced using the fabricated double-coaxial laminar flow generator. The flow rates of 200 mM CaCl<sub>2</sub> (the inlet A), the flow rate of the mixture of  $0.8 \times 10^6$  cells/mL NIH/3T3 and 1.5 wt% alginate (the inlet B), and the flow rate of 0.5 wt% alginate (the inlet C) were adjusted to 0.12 mL/min, 0.25 mL/min and 0.3 mL/min, respectively. The diameter range of the two-layered scaffolds was 570–610  $\mu\text{m}$  (Fig. 2a,b). The thickness of the hydrogel-only layer, the diffusion-restricting barrier, was approximately 100  $\mu\text{m}$  (Fig. 2a,b). The thickness range of the cell-laden layer was 120–160  $\mu\text{m}$ , based on the confocal live/dead fluorescent image (Fig. 2c,d). The diameter range of the central channel was 150–210  $\mu\text{m}$  (Fig. 2c,d). On day 1, viabilities of the nested cells were  $84.0 \pm 5.2\%$ ,  $82.2 \pm 6.1\%$  and  $86.0 \pm 5.9\%$  for the non-pumping, heartbeat-mimicking pumping and continuous pumping conditions, respectively. In order to compose the cell-laden calcium-alginate scaffold, cells were suspended in nutrient-free alginate solution inside the syringe pump for over 30 min. This may have affected the around 85% cell viability.

### Secure connection test between the composed tubular scaffold and the PDMS connector

In order to check for how long the connection setup could supply medium, the condition of the connection between the scaffold and the connector's outlet was tested under both continuous and heartbeat-mimicking pumping conditions. The outer diameter of the cell-free scaffold was 600–612  $\mu\text{m}$  and the inner diameter of the connector's outlet was 550–556  $\mu\text{m}$ . The cell-free tubular scaffold was sucked up to a point 30 mm from the end of the connector outlet. A food-dye solution was pumped until the cell-free scaffold was disconnected. The results of the disconnection test are shown in Table 1. A 10  $\mu\text{L}/\text{min}$  flow rate was applied successfully for up to 15 d, with no leakage under either pumping

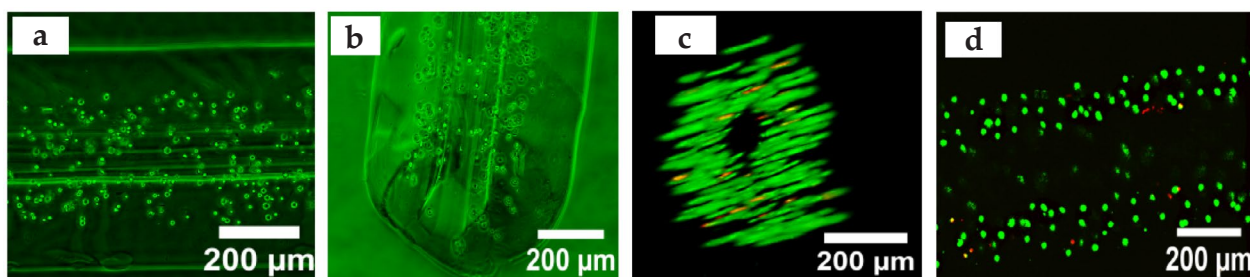


**Fig. 2. The two-layered cell-laden tubular scaffold.** (a-b) The middle and end part of the two-layered cell-laden tubular scaffold. (c-d) The cross-sectional view of the two-layered cell-laden tubular scaffold.

conditions. Over a 100  $\mu\text{L}/\text{min}$  flow rate, the scaffolds became disconnected immediately and damage occurred to the area inside the outlet of the connector because of flow pressure. At 20  $\mu\text{L}/\text{min}$ , the volumetric flow rate in a human retinal blood vessel, the continuous pumping

condition was maintained successfully for up to  $11.8 \pm 0.76$  d and the heartbeat-mimicking pumping condition for  $13.5 \pm 0.86$  d with a statistical significance of  $p < 0.05$ . This result indicated that the heart-beat mimicking condition could sustain a secure connection for longer than

**Table 1.** The elapsed time before loosening of the cell-free scaffold from the connector outlet in both pumping conditions (\* $p < 0.05$ , \*\* $p < 0.01$ ,  $n = 3$ ).

Flow rate ( $\mu\text{L}/\text{min}$ )	10	20	30	50	100
Continuous pumping	Not detaching up to 15 d	$11.8 \pm 0.33$ d *	$4.6 \pm 0.4$ d **	$2 \pm 0.4$ h *	Immediate detaching
Heartbeat-mimicking pumping	Not detaching up to 15 d	$13.5 \pm 0.83$ d *	$8.6 \pm 0.6$ d **	$4 \pm 0.7$ h *	2 min

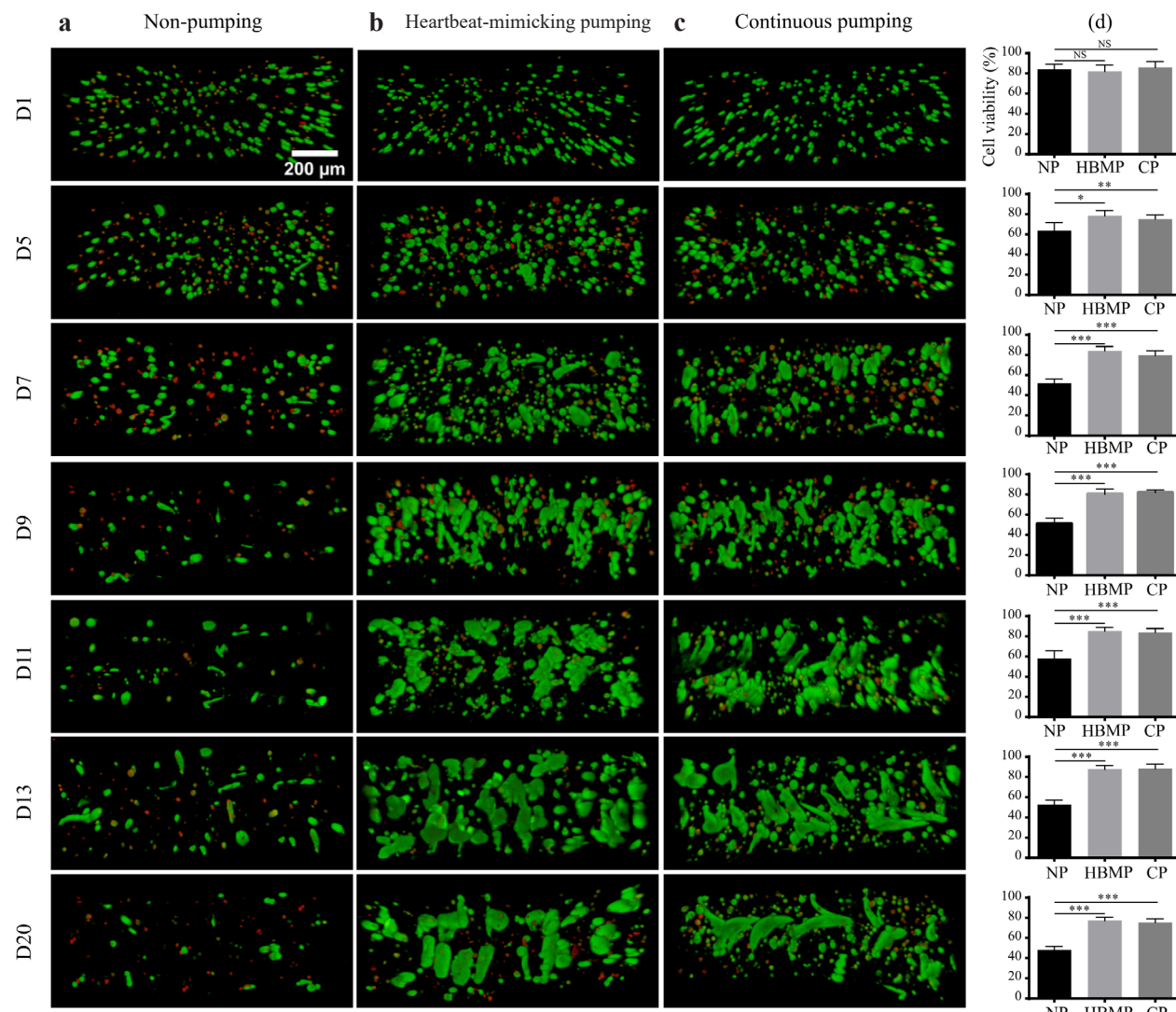


**Fig. 3.** The cell viability test according to the pumping condition. (a) The 3D confocal images of the stained NIH/3T3 cells in the two-layered tubular scaffolds in the non-pumping condition. (b) In the heartbeat-mimicking pumping condition. (c) In the continuous pumping condition. The live cells were stained as green colour by calcein-AM, and the dead cells as red by ethidium homodimer-1. (d) The cell viability comparison between three conditions at time points.

the continuous-flow condition. Because of the flow pressure, scaffolds were gradually pushed out of the outlet connector. If the tubular scaffold was sucked into the connector further than 30 mm from the outlet, the connection was maintained for a longer time (approximately 13 d).

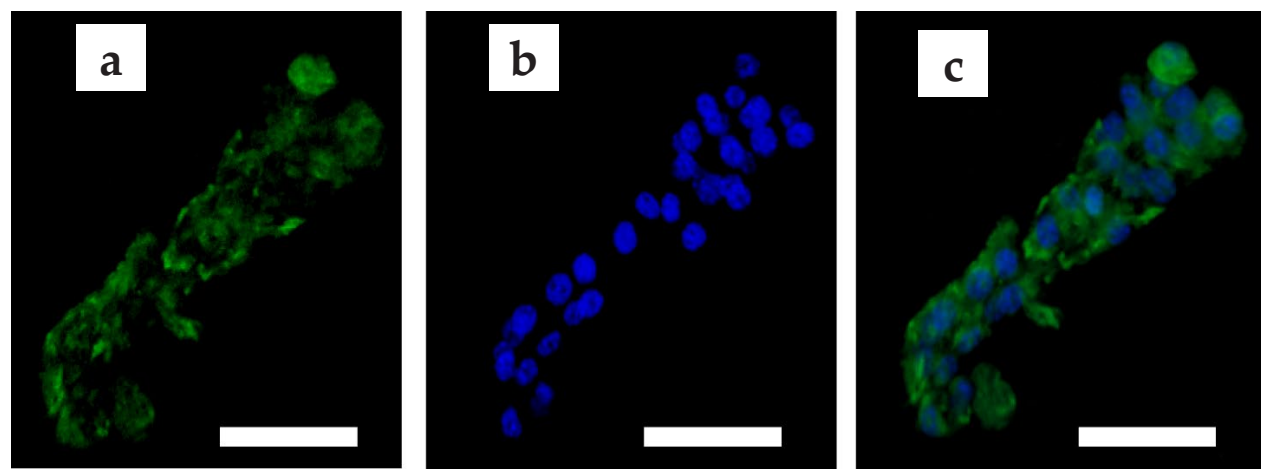
**Cell viability under the three pumping conditions**  
The live and dead NIH/3T3 cells were observed under the three different pumping conditions (Fig. 3a-c). Up until day 5, all three conditions showed a similar distribution, based on the confocal microscope images (Fig. 3a-c). Following day 5, the number of live cells started to decrease under the non-pumping condition. In contrast, cells under the other two pumping conditions maintained proliferation up to day 11. The number and area of the green colour increased gradually. No significant difference was recognised between the results for continuous pumping and the heartbeat-mimicking pumping conditions. This result indicated that cells in these fabricated scaffolds could be supplied equally with culture media. On day 12, the continuously-pumped scaffold was disconnected from the connector outlet, and on day 14, the heartbeat-mimicking pumped scaffold was disconnected. Following the disconnection, the scaffolds were simply immersed in culture media up to day 20 without any further medium pumping. The media were exchanged for fresh media every 24 h. When compared with day 13 and day 20, the numbers of live cells under the two pumping conditions decreased and dead cells increased abruptly. These observations indicated that cells could grow more successfully under the two pumping conditions.

Fig. 3d shows a cell-viability comparison between three conditions at different time points. Beginning

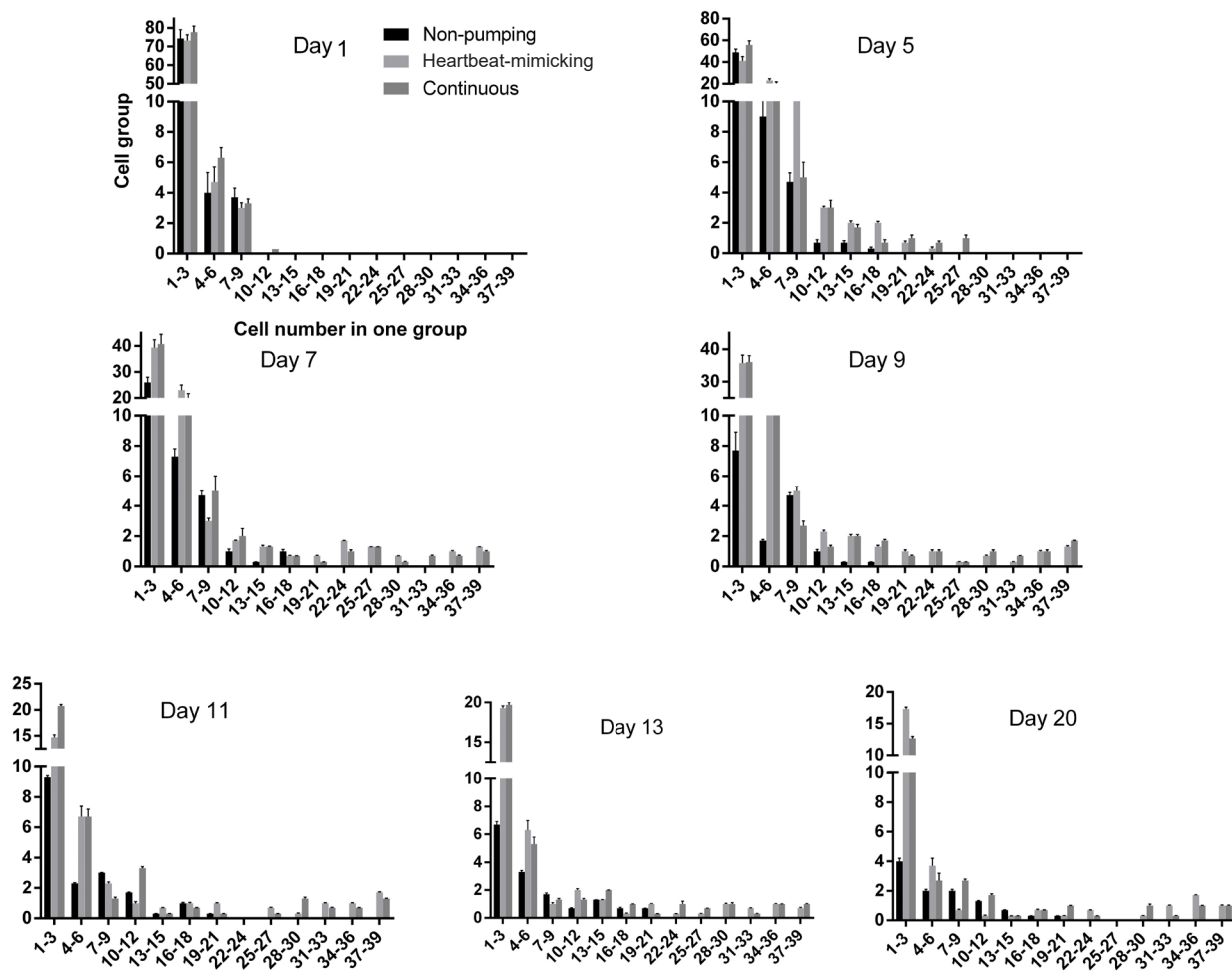
at 84.0 %, 82.2 % and 86.0 % for the continuous, heartbeat-mimicking and continuous pumping conditions, respectively, these numbers decreased considerably in all three cases up to day 5. Especially, cell viability declined 20 % under the non-pumping condition ( $^{**}p < 0.05$ ) while this change was 4 % and 9 % ( $^{**}p < 0.05$ ) under the heartbeat-mimicking and continuous condition, respectively. Following a further 2 d (day 7), only 52 % of live cells remained in the non-pumping case; whereas in contrast, it was higher than 80 % under both pumping conditions. From day 7 to day 13, there was no significant difference in cell viabilities under any of the three conditions when compared with previous time points. However, cell viability decreased significantly from day 13 to day 20 under both pumping conditions. In more detail, the cell viability declined 7 % for the heartbeat-mimicking ( $^{**}p < 0.05$ ) and 10 % for the continuous pumping condition ( $^{**}p < 0.05$ ) after one week following disconnection of the scaffold. This result demonstrated the positive effects of the two pumping conditions upon cell viability.

Fig. 4a-c show live/dead fluorescence-stained images of a cell group in the heartbeat-mimicking pumped scaffold on day 7. A  $262 \times 10^{-6} \text{ mm}^3$ -volumetric cell group was composed of 33 cells. The volume of the cell groups increased during the culture time.

In order to analyse the stained live cells quantitatively, their volumetric distribution was investigated using a three-dimensional analysis function in ImageJ. It was assumed that the volume of one NIH/3T3 cell was  $8,000 \mu\text{m}^3$  ( $20 \times 20 \times 20 \mu\text{m}$ ). Based on this assumption, the histograms of cell groups were plotted, as shown in Fig. 5. Up to day 5, all three pumping conditions showed similar numbers in the smallest cell group, having a population of 1~3 cells. Following day 7, the smallest cell group of the non-pumping condition decreased abruptly. Also,



**Fig. 4. The image of one cell group in the heartbeat-mimicking pumped scaffold.** (a) The fluorescence-stained image of the cell group in the heartbeat-mimicking pumped scaffold on day 7 was stained green by calcein-AM. (b) Nuclei were stained blue by DAPI. (c) The merged image of (a) and (b).



**Fig. 5. The frequency distribution of the cell group according to number of cells in the cell group.** The frequency of the cell groups are analysed with respect to their size (number of cells in the group) from day 1 to day 29..

the population of the largest cell group of the non-pumping condition was much smaller than that of the other two pumping conditions. On day 7, the largest volumetric cell group of the two pumping conditions, with a population of 37 ~ 39 cells, had appeared and survived until day 20, the final observation day. The largest volumetric cell group in the case of the non-pumping group had appeared by day 11, with a population of 19 ~ 21 cells, and survived until day 20.

Averaging the values over all the three pumping conditions and all the culture time, one cell group had 7.80 cells (standard deviation was 15.47). Based on this statistical analysis, the cell groups were categorised into three groups: a small group with a population of 1 ~ 3 cells, a medium group of 4 ~ 23 cells, and a large group with more than 24 cells. The distinguishing criterion between the medium group and the large group was the mean value plus one standard deviation value. The small group was defined as the smallest bin in the cell number histograms (Fig. 5). The total cell volume was the sum of the volumes of the small, medium and large groups. Fig. 6a shows total stained volume contributed to by the small, medium and large group, with respect to the three pumping conditions and the culture time. Up to day

5, all three pumping conditions showed similar total volume and similar contribution of the small and medium groups. Following day 7, the total volume under the non-pumping condition had decreased, but that of the other two pumping conditions had increased up to day 13. Following day 7, the volume contribution of the large group was over 50 % and had increased around the time of disconnection. On day 7, the largest volumetric cell group of the two pumping conditions was almost twice the volume when compared with that of the non-pumping group, as shown in Fig. 6b. Significant differences had been observed since day 7 ( $**p < 0.01$ ,  $***p < 0.001$ ). Following that, under the two pumping conditions, the volume of the largest volumetric cell group had increased gradually around the time of disconnection, and then slightly decreased on day 20.

#### Cell-cell junction assessment of the heartbeat-mimicking condition

In order to check cell-cell junctions of the NIH/3T3 cells in the two-layered tubular scaffolds, cadherins in the cell-laden scaffolds were stained and observed on day 9 of the heartbeat-mimicking condition. Fig. 7a shows cadherins (red) and nuclei (blue) of the NIH/3T3

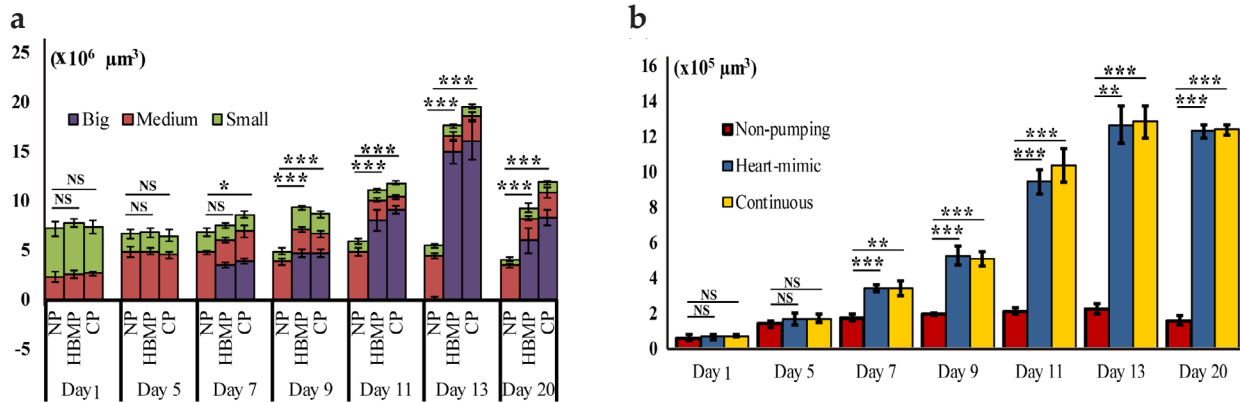


**Fig. 6. The volumetric quantification.** (a) The total volume of the live cells marked with the contribution of the small group, the medium group, and the large group (The results were obtained from 6 samples of 2 experiments). (b) The volume of the largest volumetric cell group with respect to the pumping condition and the culture time. (The results were obtained from 6 samples of 2 experiments) (\* $p < 0.05$ , \*\* $p < 0.01$ , \*\*\* $p < 0.001$ ).

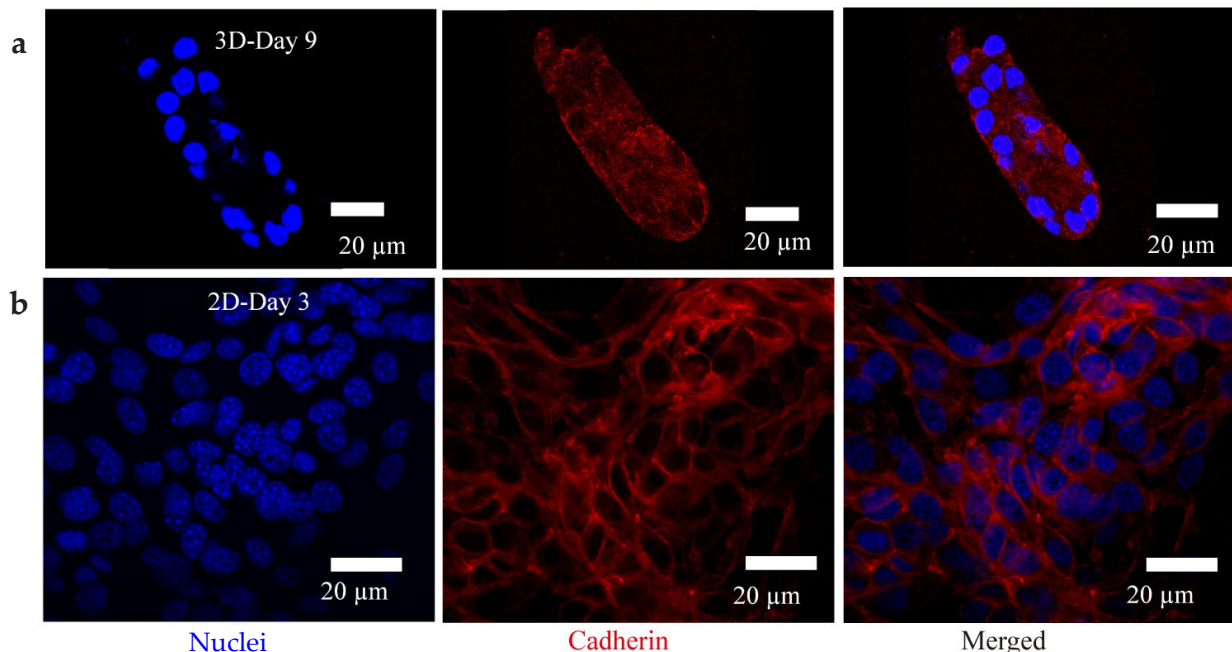


**Fig. 7. The cell-cell junction comparison between the three dimensional culturing and the two dimensional culturing.** (a) The immunofluorescent analysis of the cadherin (red) in the cell-laden scaffolds of NIH/3T3 cells with anti-rabbit cadherin antibody on day 9 of the heartbeat-mimicking pumping condition. The signal of the cadherins (red) was detected at the border of the cell-cell contact. (b) The identical analysis of NIH/3T3 cells in a conventional two-dimensional culture dish on day 3.

cells in the two-layered scaffolds. Comparing this with Fig. 7b, which were NIH/3T3 seeded in the conventional two-dimensional culture dish, cadherins appeared to be more widely distributed in the cell-laden scaffolds (Fig. 7a).

#### ECM secretion

Newly synthesised type I collagen was stained and compared to check for ECM secreted by the NIH/3T3 cells in the two-layered tubular scaffolds. In Fig. 8, the newly synthesised type I collagen is shown stained and displayed as magenta, and the nuclei as blue. Secreted type I collagen was observable on day 1. By day 7, all

the three conditions showed similar and intense staining for type I collagen. By day 10 and 20, the cells in the non-pumped scaffold did not appear to be synthesising type I collagen. In contrast, under the two pumping conditions, by day 10 the type I collagen staining was widely distributed. The staining decreased abruptly on day 20 under the two pumping conditions. This sudden decrease was expected as a result of the disconnection from the connector outlet. No significant differences were observed between the results following the use of the two different pumping conditions.

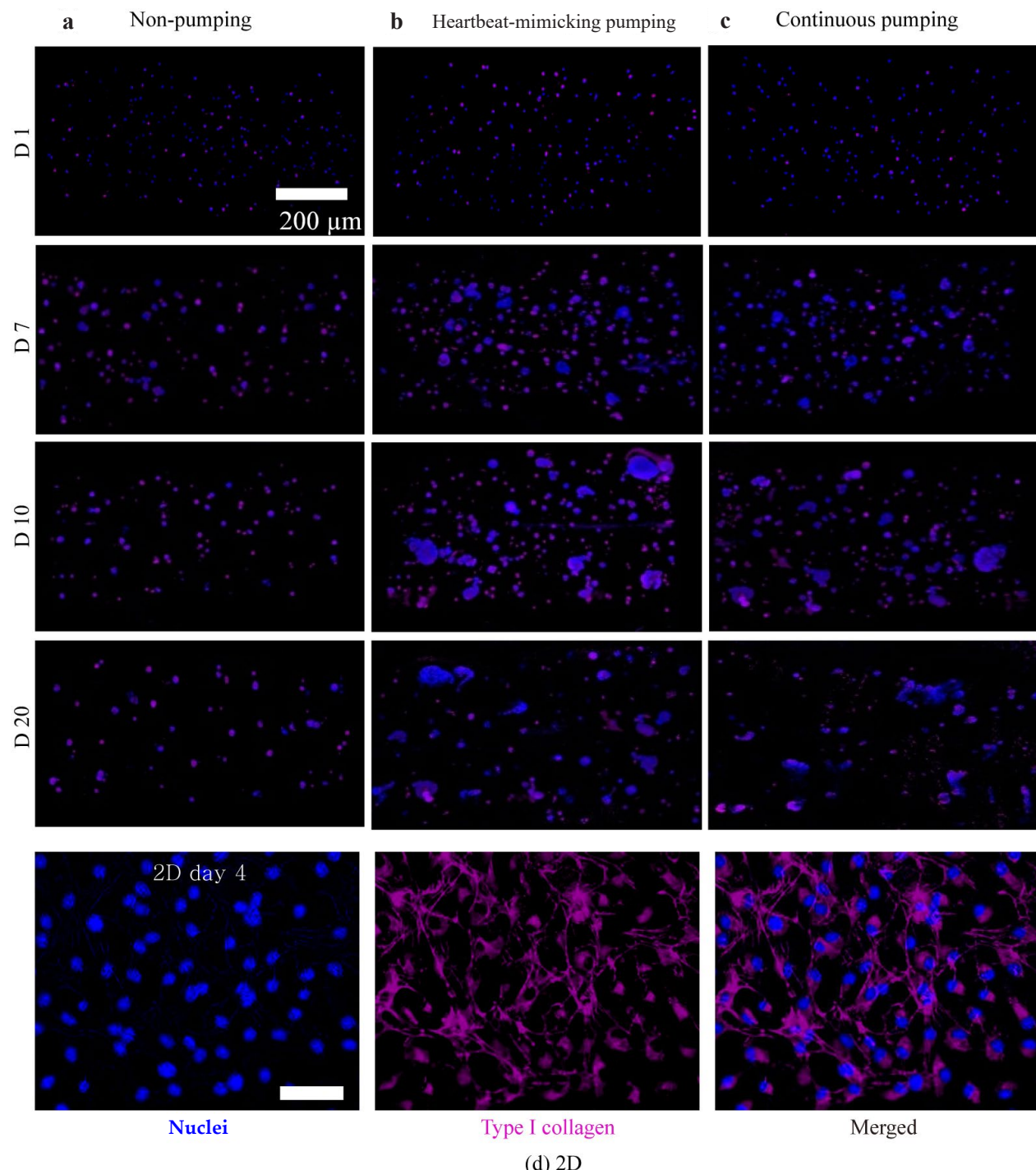


**Fig. 8. The immunofluorescent analysis of the newly synthesised type I collagen (magenta) in the cell-laden scaffolds of NIH/3T3 cells with anti-mouse type I collagen antibody. (a) at the non-pumping condition, (b) at the heartbeat-mimicking pumping condition, and (c) at the continuous pumping condition. (d) The identical analysis of NIH/3T3 cells in a conventional two-dimensional culture dish on day 4.**

## Discussion

Two-layered cell-laden tubular fibres were produced using the lab-made double-coaxial laminar flow generator. The generated cell-laden fibres were attached to an already developed PDMS connector. Using the connector, a syringe pump successfully supplied medium to the attached cell-laden tubular fibres without any

leakage for around 12 d. The transparent outer cell-free calcium-alginate layer of the tubular fibres enabled the observation of the effects of the pumped medium upon the fibre and its contents. Following the detachment of the tubular fibres from the connector on day 12 and 14, the ejected cell-laden fibres were cultured up to day 20 in order to observe effects of halting the medium pumping. The proliferation, cell-cell junction, and

newly secreted ECM were monitored with respect to the culturing time and the three different pumping conditions.

The generated scaffolds consisted of, from the inside to the outside, the core channel, the cell-laden layer and the calcium-alginate hydrogel only layer (Fig. 2a-d). Considering the distribution of cell proliferation and viability as well as the newly secreted ECM (Fig. 3a-d and Fig. 8), the calcium-alginate hydrogel only layer caused a decrease in diffusion of nutrients from the outside medium into the cell-laden layer. Lee *et al.* (2014) demonstrate medium-supplying to a tubular collagen scaffold in the absence of a secure connection, despite considerable medium leakage. Because there is no diffusion barrier layer, the cells farthest from the medium-supplying channel survive and mostly proliferate, even though they are located 4 mm away from the medium-supplying channel. In the current study, the farthest cells were about 160  $\mu\text{m}$  away and showed similar behaviour to that of the nearest cells. The supplied medium appeared to diffuse well up to distances of 160  $\mu\text{m}$ .

Jung *et al.* (2014) reported that the Young's modulus of the tubular microgels fabricated by a similar laminar-flow generator was in the range of  $9.8 \pm 1.5$  kPa to  $12.2 \pm 1.9$  kPa. Thanks to this flexibility, the two-layered scaffolds in the current study could make a secure connection with the developed PDMS micro-connector. The food dye injected from the syringe pump flowed, through the micro-connector, to the end part of the two-layered tubular scaffolds without any leakage (Fig. 1i-l).

In the durability test, using 20  $\mu\text{L}/\text{min}$  food dye, the cell-free tubular scaffolds sustained a secure connection for 11–14 d (Table 1). In the cases of 30, 50 and 100  $\mu\text{L}/\text{min}$  food dye with heartbeat-mimicking pumping, the connection endured almost twice as long as with the continuous pumping condition ( $*p < 0.05$ ,  $**p < 0.01$ ). In contrast, in the cases of 10 and 20  $\mu\text{L}/\text{min}$  food dye, the duration-time ratio between the two pumping conditions decreased dramatically. At high flow rates, the pumping volume determined the secure connection time ( $*p < 0.05$ ). At low flow rates, other factors such as degeneration of the hydrogel appear more dominant for the secure connection. In the culture-medium pumping experiment, the heartbeat-mimicking pumping condition was sustained for 14 d and the continuous pumping condition for 12 d.

These long secure connection times could support favourable conditions for proliferation, elongation and differentiation of seeded cells such as human umbilical vein endothelial cells (HUEVCs). Moreover, thanks to the simple connection configuration, it may be possible to harvest such cultured tissue-like structures for implanting. With the currently described

connection configuration, the tubular scaffolds were sucked into the connector for up to 30 mm from the end of the connector outlet. If this overlapping distance was increased, the secure connection time would also be expected to increase as well. Such an extended secure connection time would also probably expand the possible application area of the developed micro-connector.

Cell medium was pumped using three conditions: the heartbeat-mimicking pumping condition (20  $\mu\text{L}/\text{min}$  flow rate, 1 s period and 50 % pulse width), the continuous pumping condition (20  $\mu\text{L}/\text{min}$  flow rate), and the non-pumping condition. The heartbeat-mimicking condition resembled the blood flow environment in the human body (Riva *et al.*, 1985; Wang *et al.*, 2007). The two pumping conditions showed much more proliferation, higher cell viability, and much more newly secreted ECM, when compared with the non-pumping condition. No significant difference was detected between the heartbeat-mimicking pumping condition and the continuous pumping condition. The half-duty cyclic period pumping had a similar effect to the continuous pumping. This could mean that the half-duty cyclic period pumping saved half of the culture medium volume. A further, more sophisticated investigation, is required to elucidate the effects of periodic pumping.

On day 1, the viabilities of the nested 3T3 cells were  $84 \pm 5.2$ ,  $82.2 \pm 6.1$ ,  $86 \pm 5.9$  % for the non-pumping, heartbeat-mimicking pumping and continuous pumping condition, respectively, and they had started to synthesise type I collagen (Fig. 8). As time proceeded, the cell scaffold became gradually degraded and the seeded cells proliferated. From day 1 to day 5, the total volume of all the three scaffolds did not change significantly, but the distribution of the small and medium cell groups was very different (Fig. 6a). It appeared as if the seeded cells had attempted to make a tissue-like structure immediately after stabilisation. On day 7, the total volume of the non-pumped scaffold started to decrease, but that of the two pumped scaffolds started to increase (Fig. 5). This might have been the beginning of the medium-supply effect. The confocal microscope images (Fig. 2 and Fig. 3a-c) and the volumetric analysis of the cell groups (Fig. 5 and Fig. 6) indicated that the large cell group emerged in the two pumped scaffolds on day 7. The signal of the type I collagen had become stronger when compared with the previous day (Fig. 8). On day 9, at least 15 cells were observed to make junctions with each other as one cell group (Fig. 7). The continuously-pumped scaffold and the heartbeat-mimicking pumped scaffold were disconnected from the micro-connector at around day 12 and 14, respectively. Up to day 13, the live cell images of the two pumped scaffolds showed

a gradually increasing distribution (Fig. 3a-c). After the disconnection, the most volumetric cell groups of the two pumped scaffolds showed a slight decrease in volume (Fig. 5), even though their total volume had decreased abruptly (Fig. 4a). It is suggested that the tissue-like structure of the large group could more easily endure a harsh environment than the small group.

Even though animal cells do not produce endogenous alginases to enzymatically degrade alginate scaffolds (Ashton *et al.*, 2007), cell proliferation increases the cell population within the scaffold. This means that the alginate scaffold becomes less stable. Moreover, when cell scaffolds are seeded in a balanced salt solution, such as cell culture media, gradual ion reactions between  $\text{Ca}^{2+}$  and  $\text{Na}^+$  causes the cell scaffolds to be slowly degraded. To check this possibility, the mechanical strength of single-layered cell-laden tubular scaffolds was measured according to time points (details not included). The result indicated that the cell culture media and the cell proliferation reduced the durability of the alginate scaffolds. Because of this indirect assessment, it is not obvious whether NIH/3T3 cells secreted something to degrade the alginate scaffold, or not. In order to understand the specific mechanism, more sophisticated research is required.

## Conclusions

The medium-supplying system sustained with a secure connection for up to 14 d under the heartbeat-mimicking pumping condition and 12 d under the continuous-pumping condition. The initially seeded cells proliferated, adhered to each other, and made three-dimensional cell groups of over  $438 \times 10^{-6} \text{ mm}^3$  in volume. Under the pumping conditions, cells exhibited better proliferation, confluence, viability and ECM secretion. Currently, an attempt is being made to generate and culture multi-vascular engineered tissues (blood vessel, pancreas, skeletal muscle, liver tissue *etc.*) using such methods.

## Acknowledgements

This work was supported by the Ministry of Science and ICT (NRF-2017R1D1A1B03034982, and NRF-2017R1A2B4011478) and the Ministry of Health and Welfare Republic of Korea (HI19C0642).

There are no conflicts of interest to declare.

## References

- Ashton RS, Banerjee A, Punyani S, Schaffer DV, Kane RS (2007) Scaffolds based on degradable alginate hydrogels and poly(lactide-co-glycolide) microspheres for stem cell culture. *Biomaterials* **28**: 5518-5525.
- Duong VT, Dang TT, Lee Y, Nguyen CT, Phan HL, Shin D, Lee Y, Park H, Lee H, Son H, Jang H, Oh S, Back SH, Hwang C (2018) A KK cell attachment on inside-outside surface and cell encapsulation in wall of microscopic tubular scaffolds for vascular tissue-like formation. In: Proceedings of the 2018 40th annual international conference of the IEEE Engineering in Medicine and Biology Society (EMBC), pp 4198-4201.
- Folkman J (1995) Angiogenesis in cancer, vascular, rheumatoid and other disease. *Nat Med* **1**: 27-31.
- Hannoun BJM, Stephanopoulos G (1986) Diffusion coefficients of glucose and ethanol in cell-free and cell-occupied calcium alginate membranes. *Biotechnol Bioeng* **28**: 829-835.
- Jeong W, Kim J, Kim S, Lee S, Mensing G, Beebe DJ (2004) Hydrodynamic microfabrication via "on the fly" photopolymerization of microscale fibers and tubes. *Lab Chip* **4**: 576-580.
- Jung J, Kim K, Choi SC, Oh J (2014) Microfluidics-assisted rapid generation of tubular cell-laden microgel inside glass capillaries. *Biotechnol Lett* **36**: 1549-1554.
- Kim S, Chung M, Ahn J, Lee S, Jeon NL (2016a) Interstitial flow regulates the angiogenic response and phenotype of endothelial cells in a 3D culture model. *Lab Chip* **16**: 4189-4199.
- Kim S, Chung M, Jeon NL (2016b) Three-dimensional biomimetic model to reconstitute sprouting lymphangiogenesis *in vitro*. *Biomaterials* **78**: 115-128.
- Kim S, Lee H, Chung M, Jeon NL (2013) Engineering of functional, perfusable 3D microvascular networks on a chip. *Lab Chip* **13**: 1489-1489.
- Landers R, Hübner U, Schmelzeisen R, Mühlaupt R (2002) Rapid prototyping of scaffolds derived from thermoreversible hydrogels and tailored for applications in tissue engineering. *Biomaterials* **23**: 4437-4447.
- Lee VK, Kim DY, Ngo H, Lee Y, Seo L, Yoo SS, Vincent PA, Dai G (2014) Creating perfused functional vascular channels using 3D bio-printing technology. *Biomaterials* **35**: 8092-8102.
- Miller JS, Stevens KR, Yang MT, Baker BM, Nguyen DH, Cohen DM, Toro E, Chen AA, Galie PA, Yu X, Chaturvedi R, Bhatia SN, Chen CS (2012) Rapid casting of patterned vascular networks for perfusable engineered three-dimensional tissues. *Nat Mater* **11**: 768-774.
- Mori N, Morimoto Y, Takeuchi S (2017) Skin integrated with perfusable vascular channels on a chip. *Biomaterials* **116**: 48-56.
- Nguyen D-HT, Stapleton SC, Yang MT, Cha SS, Choi CK, Galie PA, Chen CS (2013) Biomimetic model to reconstitute angiogenic sprouting morphogenesis *in vitro*. *Proc Natl Acad Sci U S A* **110**: 6712.
- Oh D, Lee S, Koo KI, Seo JM (2015) Microscopic tubular cell organization for artificial vascularization. In: Lacković I, Vasic D. (eds) 6th European Conference of the International Federation for Medical and

Biological Engineering. IFMBE Proceedings, vol 45. Springer, Cham pp 322-325.

Onoe H, Okitsu T, Itou A, Kato-Negishi M, Gojo R, Kiriya D, Sato K, Miura S, Iwanaga S, Kuribayashi-Shigetomi K, Matsunaga YT, Shimoyama Y, Takeuchi S (2013) Metre-long cell-laden microfibres exhibit tissue morphologies and functions. *Nat Mater* **12**: 584-590.

Riva CE, Grunwald JE, Sinclair SH, Petrig BL (1985) Blood velocity and volumetric flow rate in human retinal vessels. *Invest Ophthalmol Vis Sci* **26**: 1124-1132.

Srigunapalan S, Lam C, Wheeler AR, Simmons CA (2011) A microfluidic membrane device to mimic critical components of the vascular microenvironment. *Biomicrofluidics* **5**: 1-9.

Tao YK, Kennedy KM, Izatt JA (2009) Velocity-resolved 3D retinal microvessel imaging using single-pass flow imaging spectral domain optical coherence tomography. *Opt Express* **17**: 4177-4188.

Vacanti JP, Langer R (1999) Tissue engineering: the design and fabrication of living replacement devices for surgical reconstruction and transplantation. *Lancet* **354**: S32-S34.

Wang Y, Bower BA, Izatt JA, Tan O, Huang D (2007) *In vivo* total retinal blood flow measurement by Fourier domain Doppler optical coherence tomography. *J Biomed Opt* **12**: 041215-041215.

White SM, Pittman CR, Hingorani R, Arora R, Esipova TV, Vinogradov SA, Hughes CCW, Choi B, George SC (2014) Implanted cell-dense prevascularized tissues develop functional vasculature that supports reoxygenation after thrombosis. *Tissue Eng Part A* **20**: 2316-2328.

Yeon JH, Ryu HR, Chung M, Hu QP, Jeon NL (2012) *In vitro* formation and characterization of a perfusible three-dimensional tubular capillary network in microfluidic devices. *Lab Chip* **12**: 2815-2815.

Zhang R, Larsen NB (2017) Stereolithographic hydrogel printing of 3D culture chips with biofunctionalized complex 3D perfusion networks. *Lab Chip* **17**: 4273-4282.

## Discussion with Reviewers

**Reviewer I:** Could the authors speculate on the potential use of this method to generate functional vessels (*i.e.* including different coaxial layers of

endothelial cells from the inner of the vessel wall, pericytes, and vascular smooth muscle cells)? Additionally, can the authors speculate on possible alternative hydrogels to be used for the fabrication of more physiologically relevant vessels (*i.e.* capable of triggering the endothelial cell self-organisation process and angiogenesis)?

**Authors** The co-axial co-culture of smooth muscle cells (the outer layer) and endothelial cells (the inner layer) would be expected to generate functional vessels. Furthermore, the method demonstrated in this study could be applied to mimic vascularised organ tissue by co-culturing endothelial cells and organ cells such as from liver. Numerous researchers have accomplished various functional hydrogels to release growth factors. Especially, Richardson and colleagues have reported PLG with VEGF and PDGF for mature vascularization in 2001. This kind of functional hydrogel could facilitate the method described in this study. Currently the authors are attempting to mimic two-layered blood vessel with SMCs and endothelial cells in mixture of alginate and collagen.

**Andrea Vernengo:** The authors highlight the significance of this work in terms of the need for a method of nutrition delivery to thick and complex tissues. The authors were successful in maintaining medium delivery and cell viability with their novel system for up to 13 d. Is this a sufficient time period for supporting the formation of vascular engineered tissue for implantation? If not, how will the authors address the need for longer term medium delivery?

**Authors:** Yeon and colleagues in 2012, reported the migration of HUVECs inside their novel microfluidic chip within 3 d. Noor and colleagues in 2019, demonstrated vessel formation of ECs inside their free-standing scaffold within 7 d. However, some other cells might need more than 13 d for maturation. For very long medium delivery, authors are attempting various methods including a smaller-diameter connector to hold the scaffold more tightly, re-inserting the detached scaffold into another smaller-diameter connector, a new connector design, and so on.

**Editor's note:** The Scientific Editor responsible for this paper was Mauro Alini.